Blends of Isotactic Polypropylenes and a Plastomer: Crystallization and Viscoelastic Behavior

María L. Cerrada, Oscar Prieto, José M. Pereña, Rosario Benavente, Ernesto Pérez*

Instituto de Ciencia y Tecnología de Polímeros (CSIC). C/ Juan de la Cierva, 3. 28006 Madrid, Spain

Summary: Blends covering the entire range of compositions of a metallocenic ethylene-1-octene, CEO, copolymer and two conventional isotactic polypropylenes, iPP, of different molecular weights have been prepared, analyzing the effect of composition and molecular weight on the crystallization (studied by DSC and X-ray diffraction) and viscoelastic behavior (DMTA). It was found that those blends rich in the iPP component show a behavior practically coincident with the weighted addition of the two components. On the contrary, significant deviations were found for the blends where the CEO copolymer is the major component. These deviations are considerably more important in the case of the blends with the iPP of higher molecular weight. Moreover, both components are not miscible, exhibiting the glass transitions of the two neat components. The area under the loss tangent curves provides a preliminary information about how the toughness is enhanced using this type of impact modifier, though it provokes a significant reduction of stiffness.

Keywords: blends, crystallization behavior, ethylene-1-octene copolymer, impact resistance, isotactic polypropylene, relaxation, stiffness

Introduction

Isotactic polypropylene, iPP, exhibits valuable properties and a very competitive price. However, its poor low-temperature fracture toughness is an important drawback for several applications, so that it is often blended with elastomeric polymer materials which improve very effectively the impact resistance of iPP. The use of single-site highly-active metallocene catalysts has allowed the synthesis of ethylene copolymers with a very homogeneous comonomer distribution and narrow molecular weight distribution. Moreover, high comonomer contents are easily incorporated, in such a way that very low density polyethylenes can be obtained, exhibiting elastomeric properties.[1,2] Therefore, these metallocene polyethylenes are good candidates for their use as impact modifiers of iPP and the properties of the corresponding blends will depend very much on crystallinity, morphology and degree of dispersion,[3] which, in turn, seems to be very much

 DOI: 10.1002/masy.200350809

affected by the polymer miscibility in the molten state.[4,5] The aim of this work is to analyze the crystallization behavior and the corresponding structural studies on blends of iPP and an ethylene-1-octene copolymer and the further influence of the macroscopic morphology on the viscoelastic mechanisms exhibited.

Experimental

The two conventional commercially available iPP's, PP1 and PP2, respectively, analyzed in the current paper have been supplied by Repsol-YPF. A commercial metallocenic catalyzed CEO copolymer with a 9.3-mol % comonomer content, was utilized in the blends and has been supplied by Exxon Chemical. Table 1 shows the characteristics of the various plain polymers.

Table 1. Sample characteristics of the commercial materials analyzed.[a]

Sample	Isotacticity (% mmmm)	Mol % 1-octene	M_w	M_w/M_n	MFI
PP1	92.6	-	224000	4.2	35
PP2	91.8	-	349000	4.0	8.5
CEO	-	9.3	115000	2.5	1.1

[a]Data supplied by the manufacturers.

Blends with different content in CEO: 25, 50, 67, 75% in weight, labeled as PP1CEO75/25, PP1CEO50/50, PP1CEO33/67, PP1CEO25/75, PP2CEO75/25, PP2CEO50/50, PP2CEO33/67 and PP2CEO25/75, respectively, were prepared in a Haake Rheocord 9000 at 210°C and at 40 rpm for 10 min. After blending and homogenization of the two components, sheets specimens were obtained as films by compression molding in a Collin press between hot plates (200°C) at a pressure of 1.5 MPa for 8 min and subsequently quenched to room temperature.

Wide-angle X-ray diffraction patterns were recorded in the reflection mode at room temperature by using a Philips diffractometer with a Geiger counter connected to a computer. Ni-filtered CuK_α radiation was used. The diffraction scans were collected over a period of 20 minutes in the range of 2θ values from 3 to 43 degrees, using a sampling rate of 1 Hz. The goniometer was calibrated with a silicon standard.

The samples were also studied by either wide, WAXS, or small-angle X-ray scattering, SAXS, employing synchrotron radiation (λ= 0.150 nm) in the beamline A2 at HASYLAB (Hamburg,

Germany). Two linear position-sensitive detectors were used. The SAXS one, at a distance of 235 cm from the sample, was calibrated with the different orders of the long spacing of rat-tail cornea (L = 65 nm). It was found to cover a spacings range from 5 to 55 nm. The WAXS detector, covering a 2θ range from about 10 to 30 degrees, was calibrated with the different diffractions of crystalline PET. A heating rate of 8°C/min was used, acquiring data simultaneously in the two detectors in time frames of 15 s.

Calorimetric analyses were carried out in a Perkin-Elmer DSC7 calorimeter, connected to a cooling system and calibrated with different standards. The sample weights ranged from 5 to 7.5 mg. A temperature range from -70°C to 200°C has been studied and the used heating rate was 20 C min^{-1}. For crystallinity determinations, values of 209 and 290 J g^{-1} have been taken as the enthalpy of fusion of a perfectly crystalline material in iPP[6] and polyethylene, PE[7], respectively.

Viscoelastic properties were measured with a Polymer Laboratories MK II dynamic mechanical thermal analyzer working in the tensile mode. The real (EÑ) and imaginary (EÕ) components of the complex modulus and the loss tangent (tan δ) of each sample were determined at 1, 3, 10 and 30 Hz, over a temperature range from -150 to 150°C, at a heating rate of 1.5°C min^{-1}.

Results and Discussion

Figure 1 shows the X-ray diffractograms, acquired at room temperature, of the different pure components and blends. The two upper patterns in both figures, corresponding to the pure iPP components, exhibit the five main diffractions characteristic of the monoclinic α modification[8,9] of iPP (the samples are commercial polymers synthesized with traditional Ziegler-Natta catalysts, and no sign of the β or γ modifications[9-11] is detected). There is, however, a noticeable difference between the diffractograms of the two iPP samples. Thus, PP1 presents approximately equal intensities for the two first reflections (110 and 040), while the 110 peak is much more intense than the other in sample PP2. This feature is in relation to the fact that the film specimens have been obtained by compression molding, and the molecular weight differences between the two iPP samples seem to lead to different degrees of orientation on the final samples. This effect becomes less important as the CEO content increases in the blends.

Regarding the diffractogram corresponding to pure CEO, it can be observed that it presents a rather low crystallinity (as corresponds to its relatively high comonomer content) and the 110 and 200 reflections characteristic of the orthorhombic modification of PE are barely seen.[12]

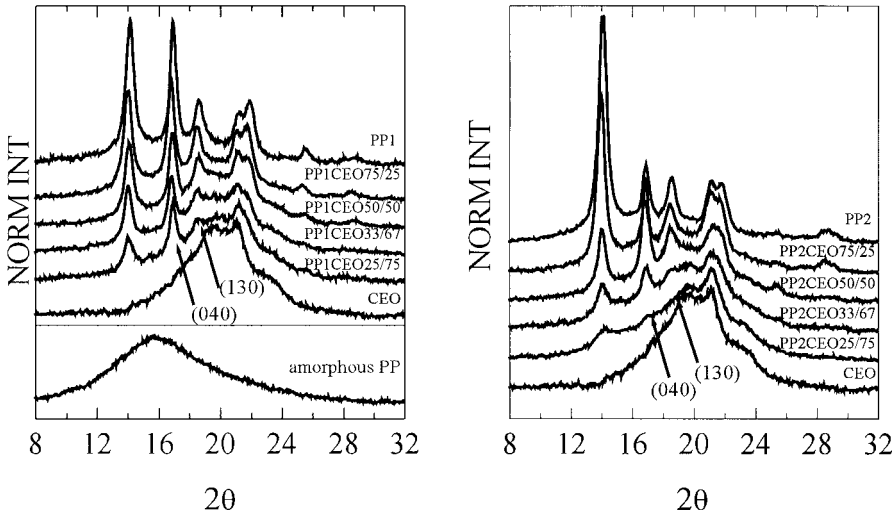

Fig. 1: X-ray diffraction patterns, at room temperature, of the different PP1/CEO (left plot) and. PP2/CEO (right plot) blends. From top to bottom (left): PP1, PP1CEO75/25, PP1CEO50/50, PP1CEO33/67, PP1CEO25/75, CEO and totally amorphous PP sample (lower frame), respectively. And, (right): PP2, PP2CEO75/25, PP2CEO50/50, PP2CEO33/67, PP2CEO25/75 and CEO, respectively.

Focusing the attention on the blends, one important difference is observed between the two kinds of blends. The experimental diffractograms of the PP1 blends practically coincide with those that can be estimated by weighting the patterns corresponding to the two pure components. On the contrary, those from PP2 lead to iPP crystallinities for the high CEO contents considerably smaller than the expected ones. This fact is reflected, for instance, in the much smaller iPP crystallinity exhibited by PP2CEO25/75 blend when compared with PP1CEO25/75. For the smaller CEO contents, however, the experimental and expected crystallinities are about the same. The iPP crystallinity in the blends can be estimated by subtracting the corresponding amounts of the CEO

profile and of the amorphous component of iPP, the latter represented by the lower diffractogram in the left plot in Figure 1 corresponding to an elastomeric, totally amorphous, PP sample.[13] After normalization to the iPP content in the blend, the normalized crystallinities are presented in Table 2 showing that crystallinity starts to diminish as CEO content increases, slightly in the blends of PP1 and rather steeply in the case of PP2.

Table 2. Normalized iPP crystallinities estimated from WAXS and DSC measurements and DSC crystallization temperatures, for the iPP component in PP1, PP2 and their corresponding blends.

Specimen	f_c^{WAXS}	f_c^{DSC}	T_c (°C)	Specimen	f_c^{WAXS}	f_c^{DSC}	T_c (°C)
PP1	0.64	0.49	115	PP2	0.61	0.49	109
PP1CEO75/25	0.64	0.48	114	PP2CEO75/25	0.61	0.46	110
PP1CEO50/50	0.64	0.48	113	PP2CEO50/50	0.61	0.44	106
PP1CEO33/67	0.61	0.61	117	PP2CEO33/67	0.43	0.35	102
PP1CEO25/75	0.57	0.41	114	PP2CEO25/75	0.20	0.14	56

Dynamic crystallization was performed by DSC, WAXS and SAXS to learn the cause of the lower crystallinity developed in PP2 blends with the highest CEO contents. The DSC curves in the left plot of Figure 2 show that the crystallization of either the PP1 or the CEO components occurs at approximately the same temperature for all compositions (around 115°C for PP1 and 56°C for CEO). On the contrary, the results for the blends of PP2 exhibit a characteristic behavior of the crystallization peak corresponding to the PP2 component. The 33% PP2 blend shows already an appreciable decrease of the crystallization temperature and that peak is absent in the case of PP2CEO25/75 (though a wide flat peak is observed with a rather small enthalpy). Moreover, it is important to note that now the exotherm corresponding, eventually, to the CEO crystallization is considerably more intense than in the case of PP1CEO25/75 (and the expectations considering the composition in CEO of that blend, i.e .75% of the enthalpy corresponding to pure CEO).

WAXS analysis at room temperature and dynamic DSC crystallization results suggest, consequently, that crystalization has been either diminished and delayed in PP2CEO33/67 and PP2CEO25/75. Then, crystllinity values are lower to those expected and crystallization occurred at lower temperature, respectively, as listed in Table 2 and Figure 2.

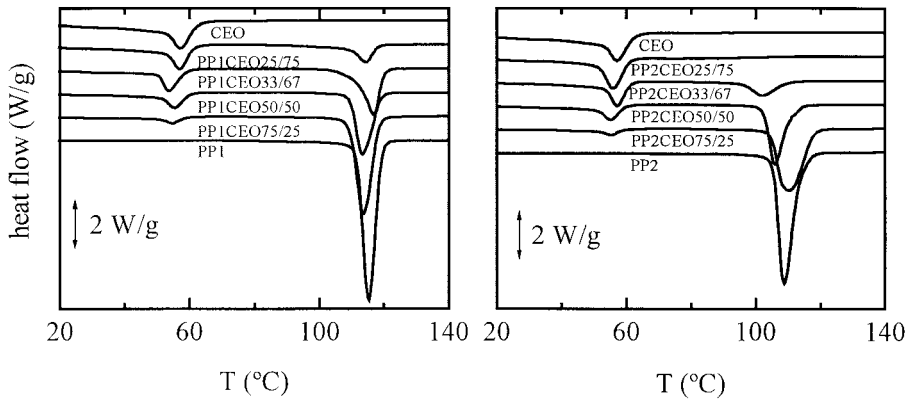

Fig. 2. DSC cooling curves corresponding to the PP1/CEO (left plot) and PP2/CEO (right plot) blends. From top to bottom (left): CEO, PP1CEO25/75, PP1CEO33/67, PP1CEO50/50, PP1CEO75/25 and PP1, and (right): CEO, PP2CEO25/75, PP2CEO33/67, PP2CEO50/50, PP2CEO75/25 and PP2, respectively.

The SAXS and WAXS results for dynamic crystallization display similar characteristics to those described for the DSC measurements in PP2CEO50/50, as depicted in Figure 3 for SAXS experiments. Each component crystallizes in their usual temperature range. However, crystallization again takes place at considerably lower temperatures in PP2CEO25/75. This feature is more clearly noticed in the analysis of the SAXS invariant,[14] as observed in Figure 4. These results reflect again that the crystallization of the iPP component in the PP2CEO25/75 blend takes place together with that for CEO. The corresponding derivative of the SAXS invariant (right plot of Figure 4) is in a very good agreement with the DSC results. The conclusion is, therefore, that the crystallization of the iPP component in the case of blend PP2CEO25/75 is considerably inhibited or, better, slowed down,[15] since it takes place at a much lower temperature, with an important proportion of iPP crystallizing simultaneously with the CEO component. An additional problem is the possibility of formation of the mesomorphic modification[14,16] of iPP instead of the regular α form. The fact that this mesomorphic modification is obtained under fast quenching conditions and that the crystallization rate of iPP in blend PP2CEO25/75 seems to be diminished considerably, opens up the possibility of formation of this mesomorphic phase.

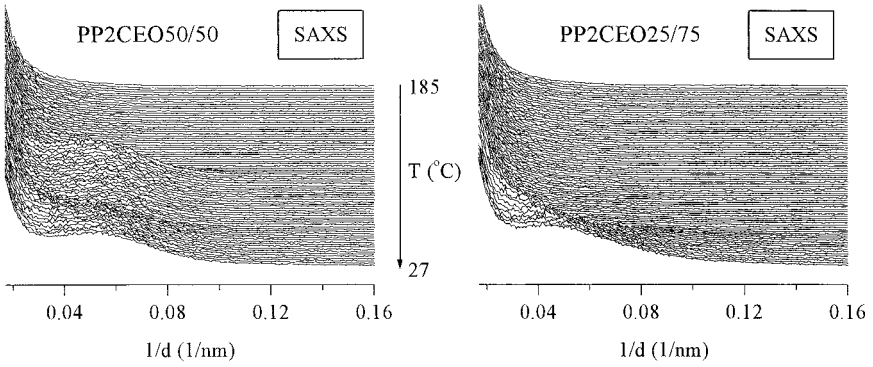

Fig. 3. Real-time SAXS profiles obtained with synchrotron radiation for PP2CEO50/50 and PP2CEO25/75 blends in a crystallization experiment at 8 °C/min.

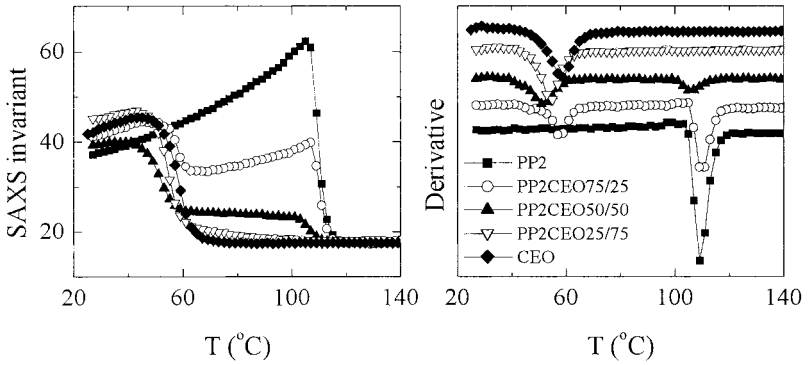

Fig. 4. Relative SAXS invariant (left plot) and derivative of the SAXS invariant (right plots) for PP2 and their respective blends with CEO.

Two different interpretations are possible to explain these results. The first one is related to the assumption that CEO is able to dissolve iPP in the molten state when the composition of iPP in the blend is low, so that the dilution effect will delay the crystallization of iPP, and only when the PE counterpart crystallizes, the iPP concentration in the non-crystalline regions will increase enough to be able to crystallize. The second interpretation is based on the supposition that the immiscible blend of these components will be subdivided into isolated regions (droplets) of small size which contain, on average, a significantly reduced number of heterogeneous nuclei where the iPP crystals

are going to grow from. Looking at the behavior of the present blends, specially that of PP2CEO25/75 (see Figure 2), and taking into account the morphology observed in an optical microscope, part of the iPP in this blend crystallizes as very small crystallites along a broad exotherm at temperatures intermediate between the exotherms of pure iPP and CEO, and another part crystallizes simultaneously with CEO. Therefore, the two interpretations given above may be occurring in the present case. The important feature to be remarked is the great influence of the molecular weight of iPP. Considering these interpretations, this effect may arise from differences in the transport term which is more significant for PP2 blends since its higher molecular weight, accentuated by the dilution effect, or, alternatively, by changes in the particle size distribution of the dispersed phase.

Figure 5 shows the viscoelastic response of PP2, CEO and their corresponding blends, which qualitatively is quite similar to that presented by blends obtained from PP1. The different relaxation processes observed are analyzed separately as follows in order of increasing temperatures.

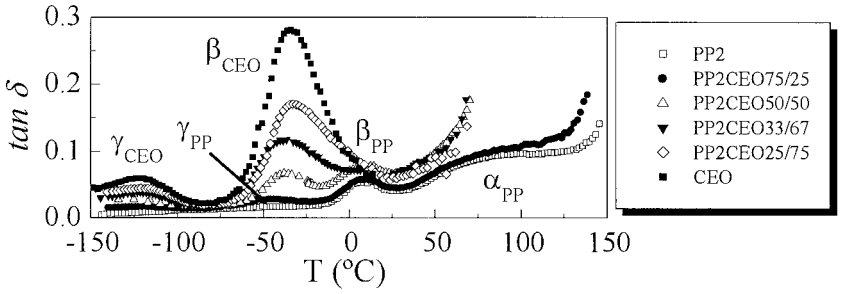

Fig. 5. Temperature dependence of the loss tangent for PP2, CEO and their blends.

The γ_{CEO} relaxation corresponds to the observed γ relaxation in polyethylene, which was firstly attributed to crankshaft movements of polymethylenic chains.[17,18] There is, however, a body of opinions which support one or more of the various model for restricted conformational transitions as kink formation, inversion and migration.[19-21] This type of motion requires chains containing sequences of three or more methylenic units. As *Figure 5* displays, the γ_{CEO} relaxation location is quite unaffected by the blend composition due to the immiscibility of the two polymers studied. In

addition, the intensity of such a process decreases and the apparent activation energy associated to it slightly increases as the iPP component increases in the blend.

The γ_{PP} relaxation, appearing around -50°C, has been attributed to local motions in the amorphous region of iPP.[22] Figure 5 shows that this relaxation is being masked in the blends by the more prominent β_{CEO} process.

The β_{CEO} relaxation corresponds to that one, which has been universally detected in branched polyethylenes at temperatures around -20°C, but it, sometimes, appears, though weakly, in some samples of linear polyethylene. Experimental evidence has been reached by DSC and MDSC about the location of the glass transition at around -48°C in the CEO and its glass fiber composites.[23] Accordingly, the β_{CEO} relaxation in CEO and in its blends with either PP1 or PP2 is considered the relaxation process associated to the glassy-rubbery transition in this component. Its location is rather independent of the type of iPP utilized for the blending.

The β_{PP} process has been identified with the glass transition temperature of the amorphous regions in iPP.[22] In the blends, as seen in Figure 5, this relaxation appears as an unambiguous peak for the PP2CEO75/25, PP2CEO50/50 blends (also in PP1CEO75/25, PP1CEO50/50, respectively). As iPP content decreases in the blend, as occurred in PP2CEO33/67, the maximum becomes a shoulder that significantly overlaps with the β_{CEO} mechanism in the side of high temperatures. Therefore, and in spite of the considerable overlapping, the two glass transitions are observed in the different blends, indicating the immiscibility of the two components.

Finally, the α_{PP} relaxation is clearly observed in the two neat iPP's and in the blends with the highest content of this component. It is attributed to movements in the iPP crystalline regions.[22] As the CEO content increases in the blends under study, the mechanical strength at temperatures higher than room temperature considerably diminishes and this motion cannot be detected. Accordingly, the tan δ parameter starts to increase without showing the characteristic shoulder exhibited by this relaxation.

A rough estimation of the impact strength can be obtained from the area under the loss tangent curve.[24] Such estimation has been made for the present samples by integration from -150°C to 30°C. The corresponding results for the PP1 blends are shown in Figure 6 as a function of the storage modulus of the sample. It can be observed that the incorporation of the plastomer leads to

a significant increase on the impact resistance, although it is accompanied by a rather pronounced diminishment on the storage modulus.

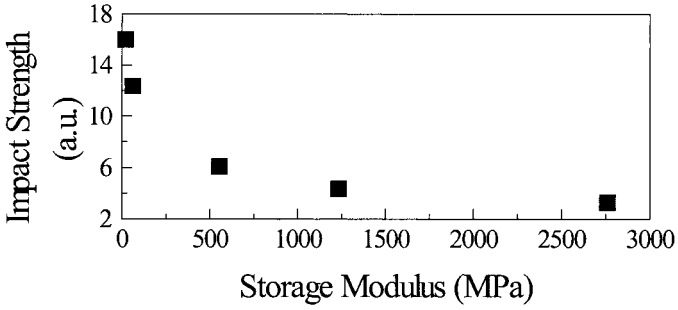

Fig. 6. Variation of the toughness (estimated by integration under the loss tangent curve) and storage modulus in iPP1, CEO and their blends.

Conclusions

The current study has established a diminishment in crystallinity and crystallization temperature corresponding to the iPP component in PP2CEO25/75 and PP2CEO33/67 blends compared with their homologous PP1CEO25/75 and PP1CEO33/67. These features point out an inhibition of the crystallization process of the iPP component in the case of the blends rich in CEO. This inhibition is considerably more pronounced for the PP2 blends. The existence of two independent glass transitions indicates immiscibility of the two components in the two kinds of blends. Moreover, the area under the loss tangent curve is considerably increased as CEO content does in the blend, pointing out an enlargement in the impact strength though it is accompanied by a clear decrease on the storage modulus. Consequently, depending upon the final requirements for a specific application, the balance between stiffness and toughness has to be found.

Acknowledgments

The financial support of CAM (Project 07G/0038/2000) and Ministerio de Ciencia y Tecnología (projects MAT2001-2321 and MAT2001-1731) and the supply of the samples by Repsol-YPF and EXXON Chemical are gratefully acknowledged. M.L. Cerrada is grateful to CSIC (I3P Programme) for her financial support. The synchrotron work (in the polymer line of Hasylab at DESY, Hamburg) was supported by the IHP Programme "Access to Research Infrastructures" of

the European Commission (Contract HPRI-CT-1999-00040). We thank the collaboration of the Hasylab personnel, and specially Dr. S. Funari and Dr. A. Meyer, responsibles of the polymer beamline.

[1] S. Bensason, J. Minick, A. Moet, S. Chum, A. Hiltner, E. Baer, *J. Polym. Sci.:Polym. Phys.* **1996**, *34*, 301.
[2] S. Vanden Eynde, V. B. F. Mathot, M. H. J. Koch, H. Reynaers, *Polymer* **2000**, *41*, 4889.
[3] A. Galeski, Z. Bartzak, M. Pracella, *Polymer* **1984**, *25*, 1323
[4] M. Yamaguchi, K.-H. Nitta, H. Miyata, T. Masuda, *J. Appl. Polym. Sci.* **1997**, *63*, 467.
[5] J. H. Lee, J. K. Lee, K. H. Lee, C. H. Lee, *Polymer J.* **2000**, *32*, 321.
[6] J. R. Isasi, L. Mandelkern, M. J. Galante, R. G. Alamo, *J. Polym. Sci., Polym. Phys.* **1999**, *37*, 323.
[7] B. Wunderlich, in "*Macromolecular Physics*", Academic Press, New York, 1980.
[8] G. Natta, P. Corradini, *Nuovo Cimento Suppl.* **1960**, *15*, 40.
[9] A. Turner-Jones, J. M. Aizlewood, D. R. Becket, *Makromol. Chem.* **1964**, *75*, 134.
[10] S. V. Meille, D. R. Ferro, S. Brückner, *Macromol. Symp.* **1995**, *89*, 499.
[11] E. Pérez, D. Zucchi, M. C. Sacchi, F. Forlini, A. Bello, *Polymer* **1999**, *40*, 675.
[12] M. L. Cerrada, R. Benavente, E. Pérez, *J. Mater. Res.* **2001**, *16*, 1103.
[13] S. Mansel, E. Pérez, R. Benavente, J. M. Pereña, A. Bello, W. Röll, R. Kirsten, S. Beck, H.-H. Brintzinger, *Macromol. Chem. Phys.* **1999**, *200*, 1292
[14] W. J. O'Kane, R. J. Young, A. J. Ryan, W. Bras, G. E. Derbyshire, G. R. Mant, *Polymer* **1994**, *35*, 1352.
[15] J. Li, R. A. Shanks, R. H. Olley, G. R. Greenway, *Polymer* **2001**, *42*, 7685.
[16] R. Androsch, B. Wunderlich, *Macromolecules* **2001**, *34*, 5950.
[17] T. F. Schatzki, *J. Polym. Sci.* **1962**, *57*, 496.
[18] R. F. Boyer, *Rubb. Chem. Technol.* **1963**, *36*, 1303.
[19] R. H. Boyd, R. S. Breitling, *Macromolecules* **1974**, *7*, 855.
[20] R. H. Boyd, *J. Polym. Sci, Polym. Phys.* **1975**, *13*, 2345.
[21] N. J. Heaton, R. Benavente, E. Pérez, A. Bello, J. M. Pereña, *Polymer* **1996**, *37*, 3791.
[22] C. Jourdan, J. Y. Cavaille, J. Perez, *J. Polym. Sci.: Polym. Phys.* **1989**, *27*, 2361.
[23] M. L. Cerrada, R. Benavente, E. Pérez, J. Moniz-Santos, M. R. Ribeiro, *Polymer* **2001**, *42*, 7197.
[24] S. H. Jafari, A. K. Gupta, *J. Appl. Polym. Sci.* **2000**,*78,* 962.